NASA TECHNICAL NOTE

NASA TN D-7356

NASA TN D-7356

FRICTION LOSSES IN A LUBRICATED THRUST-LOADED CAGELESS ANGULAR-CONTACT BEARING

by Dennis P. Townsend, Charles W. Allen, and Erwin V. Zaretsky

Lewis Research Center
Cleveland, Ohio 44135

NATIONAL AERONAUTICS AND SPACE ADMINISTRATION • WASHINGTON, D. C. • JULY 1973

1. Report No.	2. Government Accession No.	3. Recipient's Catalog No.
NASA TN D-7356		

4. Title and Subtitle	5. Report Date
FRICTION LOSSES IN A LUBRICATED THRUST-LOADED CAGELESS ANGULAR-CONTACT BEARING	July 1973
	6. Performing Organization Code

7. Author(s)	8. Performing Organization Report No.
Dennis P. Townsend, Charles W. Allen, and Erwin V. Zaretsky	E-7284
	10. Work Unit No. 501-24

9. Performing Organization Name and Address	11. Contract or Grant No.
Lewis Research Center National Aeronautics and Space Administration Cleveland, Ohio 44135	
	13. Type of Report and Period Covered
12. Sponsoring Agency Name and Address	Technical Note
National Aeronautics and Space Administration Washington, D.C. 20546	14. Sponsoring Agency Code

15. Supplementary Notes

16. Abstract

The NASA spinning torque apparatus was modified to measure the spinning torque on a cageless ball thrust bearing. Friction torque was measured for thrust loads varying from 44.5 to 403 newtons (10 to 90 lb) at speeds of 1000, 2000, and 3000 rpm. Tests were conducted with di-2-ethylhexyl sebacate and a synthetic paraffinic oil. These tests were run with either oil jet lubrication or with a thin surface film of lubricant only. An analytical model which included rolling resistance was developed and extended from previous models for spinning torque and lubricant rheology. The model was extended by the inclusion of rolling resistance. The computed values were in fair agreement with the experimental results and confirmed previous hypotheses that a thin lubricant film gives minimum bearing torque and an oil jet flow of a viscous lubricant will result in considerable rolling torque in addition to the torque due to ball spin.

17. Key Words (Suggested by Author(s))	18. Distribution Statement
Elastohydrodynamic; Spinning torque; Angular contact bearing; Bearing torque; Di-2-ethylhexyl sebacate; Synthetic paraffinic; Lubricant rheology	Unclassified - unlimited

19. Security Classif. (of this report)	20. Security Classif. (of this page)	21. No. of Pages	22. Price*
Unclassified	Unclassified	35	$3.00

* For sale by the National Technical Information Service, Springfield, Virginia 22151

FRICTION LOSSES IN A LUBRICATED THRUST-LOADED CAGELESS ANGULAR-CONTACT BEARING

by Dennis P. Townsend, Charles W. Allen*, and Erwin V. Zaretsky

Lewis Research Center

SUMMARY

The NASA spinning torque apparatus was modified to measure the spinning torque in a cageless ball thrust bearing. Friction torque was measured for thrust loads ranging from 44.5 to 403 newtons (10 to 90 lb) at speeds of 1000, 2000, and 3000 rpm. Tests were conducted with a di-2-ethylhexyl sebacate and a synthetic paraffinic oil. These tests were run with either oil jet lubrication or with a thin surface film of lubricant. An analytical model which included rolling resistance was developed and extended from a previous model for spinning torque and lubricant rheology.

The analytical and lubricant rheology models developed for calculating the friction torque in a thrust loaded ball bearing show close agreement between the computed and experimental results. For a lubricant of relatively low viscosity such as di-2-ethylhexyl sebacate, the largest contribution to the friction torque is the ball spinning component. The torque appears to be relatively unaffected by the amount of lubricant present.

For a viscous lubricant such as the synthetic paraffinic oil, the largest contribution to the friction torque is that of the rolling resistance of the balls through the lubricant. In this case, a reduction of the amount of lubricant present appreciably reduces the friction torque. With only a thin film, the contribution of the rolling resistance disappears altogether.

With a low viscosity lubricant an excess amount of lubricant present in the bearing has little deleterious effect. However, with a viscous lubricant, a nominal flow of oil to the bearing can result in a tenfold increase in the friction torque as compared with the minimum value.

---

* Professor of Mechanical Engineering, University of California, Chico, California.

INTRODUCTION

In bearing and gear applications considerable power losses occur in the systems even though good lubrication is present. In rolling element bearings these power losses result in heat generation and increase the temperature of both bearing components and lubricant. These losses occur due to a number of factors; shearing of the lubricant in the bearing cavities, rubbing of the balls and cage (separator), cage drag, spinning and rolling of the balls in the raceways and churning of the lubricant. Ball bearing kinematics are also affected by these losses. Early analytical work (refs. 1 to 3) on power losses in ball bearings were restricted to the use of Coulomb friction at the sliding contacts. More recently it has become evident that the Coulomb friction model is inadequate to completely describe all the conditions in a real bearing (refs. 4 and 5). In the later analysis (ref. 5), the elastohydrodynamic (EHD) lubricant film and the rheological properties of the lubricant were used to determine bearing friction and kinematics. The method of reference 5 uses an exponential model for the lubricant pressure-viscosity characteristics which may, however, predict power losses higher than those which generally occur in practice.

The torque of a ball spinning in a groove with different conformities and several lubricants was measured (refs. 6 to 8) in the NASA spinning torque apparatus. Later, an analytical model was developed (refs. 9 and 10) which predicted the extent that EHD film contributed to the effective ball/race separation and spinning torque. The analyses showed that conventional EHD lubrication is possible in the case of a groove having conformities up to 60 percent. The analytical model reported in references 8 and 9 was further refined by the development of a new lubricant rheological model (ref. 11). In a bearing application, however, the balls are simultaneously rolling, spinning, and plowing through lubricant, all of which contribute to the frictional forces on the balls and the complete bearing.

In view of the aforementioned, the objectives of the research reported herein are (1) to measure experimentally the power losses in a thrust loaded ball bearing without a cage, (2) to extend the previously developed analytical techniques for determining power losses of a ball spinning in a nonconforming groove to the case of a bearing operating with combined spinning and rolling, and (3) to determine analytically the effect of lubricant viscosity and aerodynamic drag on bearing power losses. Tests were conducted in the NASA spinning torque apparatus at room temperature using a cageless 204-size angular-contact ball bearing having three balls. Test conditions were 1000, 2000, and 3000 rpm and varying loads from 44.5 to 403 newtons (10 to 90 lb) with two bearings. One bearing had a 26° contact angle with a 52 percent conformity at inner and outer races. The second bearing had a 17° contact angle with 53 and 54 percent conformity at the inner and outer races, respectively. The tests were conducted with two lubricants, a di-2-ethylhexyl sebacate, and a synthetic paraffinic oil.

APPARATUS, LUBRICANTS, AND SPECIMENS

Spinning Torque Apparatus

A modification of the spinning torque apparatus (see fig. 1) as reported in references 6 and 7 was used for the tests reported herein. The apparatus essentially consists of a turbine drive, a pneumatic load device, an angular-contact test bearing, a lower test-housing assembly incorporating a hydrostatic air-bearing, and a torque-measuring system. In operation, the inner ring is pneumatically thrust loaded against the outer ring through the drive shaft. As the drive shaft is rotated, the inner ring rotates with respect to the outer ring. The friction torque on the outer ring causes an angular deflection of the lower test-specimen housing. This angular movement which is limited by a torsion wire is sensed optically by the torque-measuring system and is converted into a torque value. During a test, the torque is continuously recorded on a strip chart.

Test Bearings

The test bearings were conventional angular contact bearings with the cages and all but three balls removed. Specifications of the bearings are given in the following table:

Type	A	B
Inside diameter, mm (in.)	20 (0.7874)	20 (0.7874)
Outside diameter, mm (in.)	47 (1.8504)	47 (1.8504)
Width, mm (in.)	14 (0.5512)	14 (0.5512)
Pitch, mm (in.)	35.5 (1.309)	35.5 (1.309)
Nominal contact angle, deg	26	17
Inner race curvature, percent	52	53
Outer race curvature, percent	52	54
Number of balls	3	3
Ball diameter, mm (in.)	7.15 (0.281)	7.15 (0.281)
Hardness of inner race, R_c	62 to 64	62 to 64
Hardness of outer race, R_c	62 to 64	62 to 64
Hardness of balls, R_c	62 to 64	62 to 64
Surface finish of races, μm (μin.)	0.15 (6)	0.15 (6)
Surface finish of balls, μm (μin.)	0.025 to 0.05 (1 to 2)	0.025 to 0.05 (1 to 2)

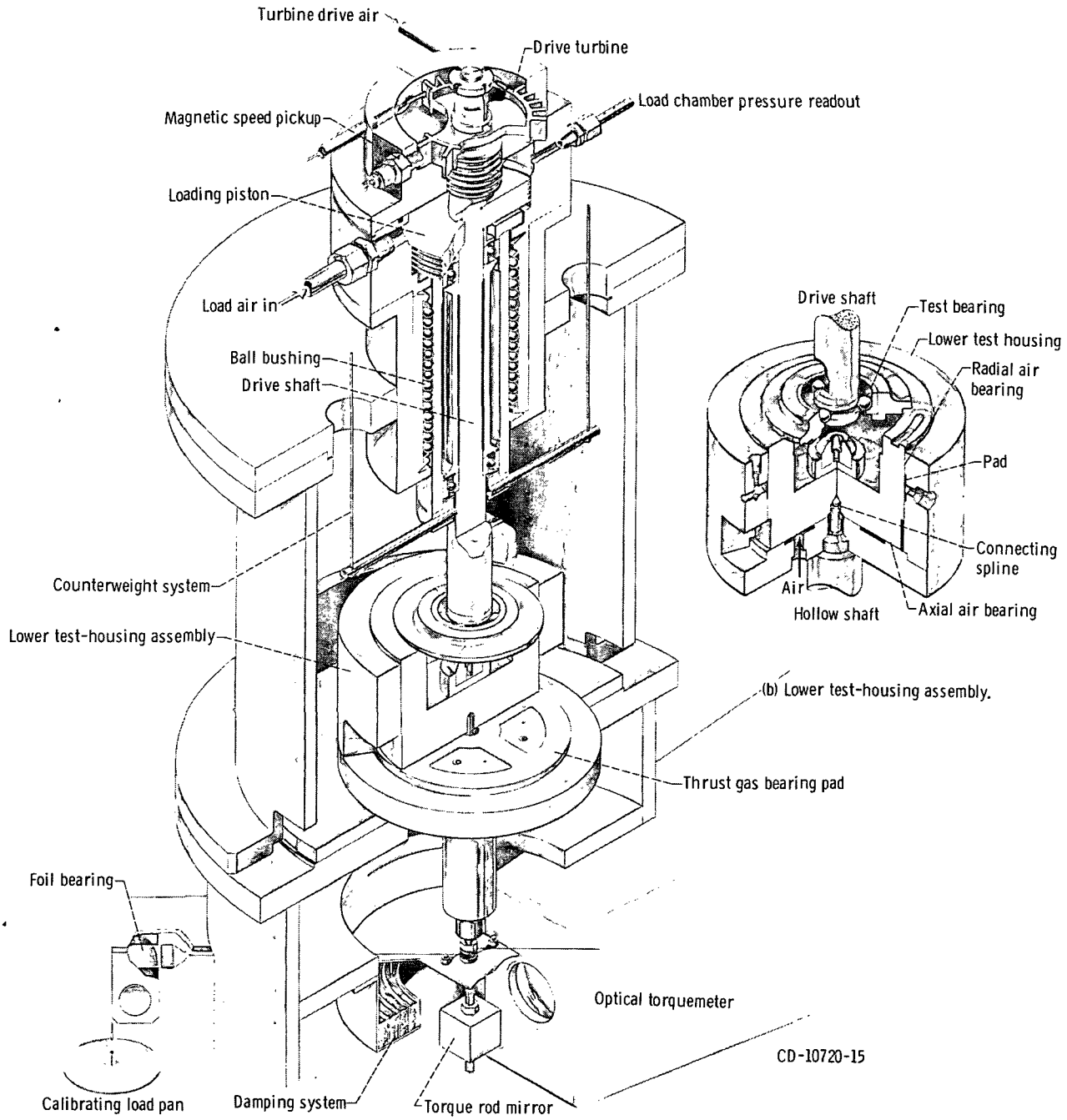

(a) General cutaway view.

Figure 1. - Bearing torque apparatus.

Lubricants

The lubricants used for the tests were as follows:

(1) Di-2-ethylhexyl sebacate with properties at 294 K (70° F) given by reference 11 as

Ambient viscosity, μ_o, N-sec/m^2 (lb-sec/in.^{2})	16×10^{-3} (2.3×10^{-6})
Pressure-viscosity exponent, α, m^2/N (psi^{-1})	1.4×10^{-8} (1.0×10^{-4})
Transition shear stress, τ_c, N/m^2 (psi)	6.89×10^6 (1000)
Lubricant factor, F	0.045

(2) Synthetic paraffinic lubricant with properties at 294 K (70° F) given by reference 11 as

Ambient viscosity, μ_o, N-sec/m^2 (lb-sec/in.^{2})	0.414 (6×10^{-5})
Pressure-viscosity exponent, α, m^2/N (psi^{-1})	1.33×10^{-8} (9.2×10^{-5})
Transition shear stress, τ_c, N/m^2 (psi)	6.89×10^6 (1000)
Lubricant factor, F	0.07

Test Procedure

Two angular-contact 204-size ball bearings with 17° and 26° contact angles were run, without a cage and with only three balls, in a bearing torque apparatus described initially in reference 8 and shown in figure 1. Tests were run to measure bearing outer-race torque at 1000, 2000, and 3000 rpm at loads from 44.5 to 403 newtons (10 to 90 lb). The bearings were run with two lubricants, a di-2-ethylhexyl sebacate and a synthetic paraffinic oil, under two different lubricant conditions. The bearings were first run with an oil jet of lubricant of approximately 8 cubic centimeters per minute and after being cleaned were lubricated by applying a few drops of lubricant which had been diluted by a 5 to 1 addition of hexane. As the lubricant solution was applied, the hexane evaporated leaving only a thin film of lubricant on the bearing surfaces. Each load and speed condition was run only long enough to reach equilibrium conditions usually 5 to 15 seconds.

ANALYSIS

Kinematics

The analysis is based upon an idealized model in which the bearing is subjected to an axial load which is distributed uniformly among the balls. Since the test specimens contain only three balls, the preceding is a realistic assumption.

In order to simplify the analysis, the ball/race interaction will be considered in relation to a coordinate system (fig. 2) which is rotating at an angular velocity Ω_c corresponding to the orbital speed of the balls. The origin of this moving system is coincident with the ball center.

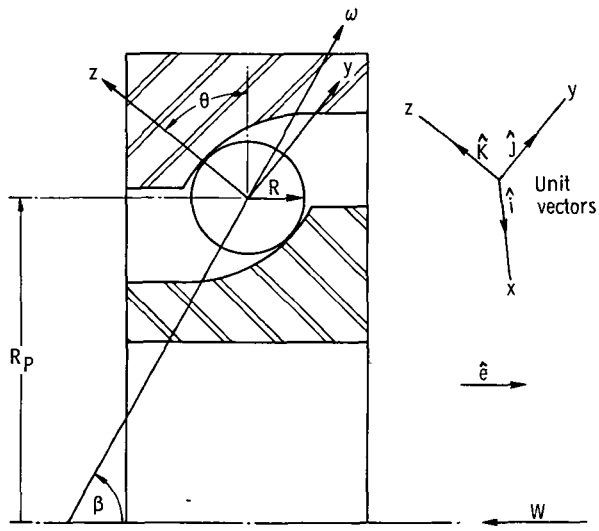

Figure 2. - Section of bearing showing coordinate system used in kinematic analysis.

The following assumptions are made in deriving the various kinematic relations:

(1) The speed is low so that inertia effects are negligible and therefore the inner and outer race contact angles are equal.

(2) The ball motion is assumed to be such that there is no slip at the nominal point contacts between ball and races. Spinning can, however, occur at both ball/race contacts.

On the basis of the preceding assumptions the rolling and spinning angular velocities can be obtained from the relation in appendix A as

$$\vec{\omega}_{ri} = -\frac{R_p}{R}\frac{\Omega_i}{2}\left[1 - \left(\frac{R}{R_p}\cos\theta\right)^2\right]\hat{j} \tag{1a}$$

$$\vec{\omega}_{ro} = -\frac{R_p}{R}\frac{\Omega_i}{2}\left[1 - \left(\frac{R}{R_p}\cos\theta\right)^2\right]\hat{j} \tag{1b}$$

$$\vec{\omega}_{si} = \frac{\Omega_i}{2}\left(1 + \frac{R}{R_p}\cos\theta\right)\left[\left(\cos\theta - \frac{R_p}{R}\right)\tan(\beta - \theta) + \sin\theta\right]\hat{k} \tag{1c}$$

$$\vec{\omega}_{so} = -\frac{\Omega_i}{2}\left(1 - \frac{R}{R_p}\cos\theta\right)\left[\left(\cos\theta + \frac{R_p}{R}\right)\tan(\beta - \theta) + \sin\theta\right]\hat{k} \tag{1d}$$

The loaded contact angle θ is dependent upon load and is computed as indicated in appendix B.

The angle β which the angular velocity vector of the balls makes with the bearing axis is a variable which is dependent upon the kinetics of the ball motion. If inertia forces are neglected, the magnitude of β is influenced mainly by the spinning torque at the inner and outer ball/race contacts.

Origin of Friction Torque

In a lubricated ball bearing, there is an EHD film between each race and ball and there is also some lubricant surrounding the high pressure EHD region. Among the possible sources of bearing friction, in a cageless thrust bearing of the type under investigation, are the following:

(1) Spinning friction arising within the EHD region

(2) Spinning friction due to the lubricant outside of this region

(3) Rolling resistance due to the lubricant being squeezed out in front of the rolling ball

(4) Friction due to translational sliding in the EHD region

(5) Fluid dynamic drag of the balls as they orbit about the center of the bearing

(6) Hysteresis losses due to elastic deformation of steel during rolling

The contribution to the bearing torque of each of these effects will be considered independently and then the total bearing torque obtained by the summation of the individual contributions. For the first order computation, coupling between the various effects will be neglected.

Spinning Torque

Analysis of the spinning torque is an extension of the work undertaken previously for the spinning of a ball in a nonconforming groove (refs. 9 and 10). The contact ellipse for the ball/race interface is shown in figure 3. As in the case of the pure

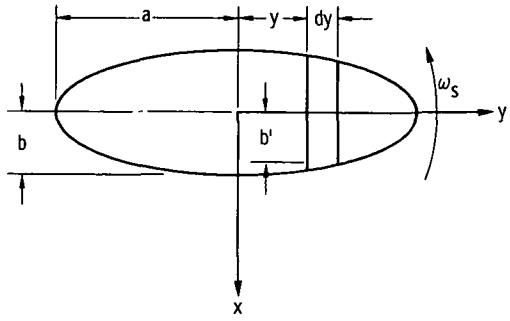

Figure 3. - Contact ellipse between ball and race.

spinning reported in references 9 and 10, several simplifying assumptions are made as follows:

(1) The stress distribution is Hertzian.

(2) The major axis of the ellipse is assumed to be considerably greater than the minor axis. For a 54 percent conformity the ratio of the major to minor axis is 5.2. For conformities less than 54 percent this ratio is larger.

(3) The major axis of the contact ellipse is considerably less than the ball radius so that the ellipse may be approximated by a plane ellipse lying in the x-y plane.

(4) The significant velocities, as far as film thickness and torque are concerned, are those in the x direction. This follows from the second assumption.

(5) The nonsymmetry of the film thickness in the positive and negative y direction is assumed to be small so that moments can be assumed to be balanced about the z axis.

(6) The surface roughness is assumed small in comparison with the thickness of the EHD film.

(7) Frictional resistance is entirely due to viscous shear.

(8) Side leakage is neglected.

(9) Rheological properties of the lubricant are as defined in reference 11.

(10) The film thickness in the x direction is constant.

(11) The surfaces are isothermal.

On the basis of the preceding assumptions, the system can be reduced to a number of elemental rollers of width dy in rolling and sliding motion relative to the groove

(fig. 3). Relative to the rotating coordinate system the surface velocity of the elemental roller is obtained in appendix A for the inner race as:

$$U_{Bi} = -\left(\omega_{ri}R + \omega_{si}y\right) \tag{2a}$$

and for the outer race as:

$$U_{Bo} = \left(\omega_{ro}R - \omega_{so}y\right) \tag{2b}$$

The magnitude of the respective surface velocities of the inner and outer races with respect to the rotating coordinate systems are:

$$U_{Ri} = \omega_{ri}R \tag{3a}$$

$$U_{Ro} = \omega_{ro}R \tag{3b}$$

The slip velocity of the ball with respect to the inner race from appendix A is obtained as

$$U_{si} = -\omega_{si}y \tag{3c}$$

and for the outer race

$$U_{so} = -\omega_{so}y \tag{3d}$$

The tractive force on each element of the contact ellipse is then given as

$$\vec{dF} = \int_{-b'}^{b'} \tau \, dx \, dy \, \hat{i} \tag{4}$$

For a Newtonian fluid with a linear velocity gradient

$$\tau = \mu \frac{U_s}{h} \tag{5}$$

where the film thickness h is given in reference 12 as

$$h = \frac{1.6\,\alpha^{0.6} E'^{0.03} R_e^{0.43} \mu_o^{0.7}}{W^{0.13}} \left(\frac{U_B + U_R}{2}\right)^{0.7} \tag{6a}$$

and

$$E' = \frac{2}{\left(\frac{1 - \nu_1^2}{E_1} + \frac{1 - \nu_2^2}{E_2}\right)} \tag{6b}$$

$$R_e = \frac{RR_R}{R + R_R} \tag{6c}$$

$$W = \frac{0.75P}{a}\left[1 - \left(\frac{y}{a}\right)^2\right] \tag{6d}$$

According to reference 11 the assumption of Newtonian behavior for the lubricant is not realistic at high pressures and shear rates and a more general model is

$$\tau = \mu_o e^{\alpha s} \frac{U_s}{h} \qquad \tau < \tau_c \tag{7a}$$

$$\tau = \mu_o e^{\alpha s} \frac{U_s}{h} \qquad \tau_c < \tau < Fs \tag{7b}$$

$$\tau = Fs \qquad \mu_o e^{\alpha s} \frac{U_s}{h} > Fs \tag{7c}$$

The computation of τ using the foregoing relations proceeds as follows:

(1) At a given value of y the film thickness is computed using equation (6a).

(2) For each value of x at the given value of y the Hertzian contact pressure is given by

$$s = \frac{1.5P}{\pi ab}\left(1 - \frac{y^2}{a^2} - \frac{x^2}{b^2}\right)^{1/2} \tag{8}$$

The shear stress τ is then computed by equation (7a) and then, if it is larger than τ_c and also larger than F_s, it is recomputed by equation (7c) but the sign remains the same as in the original computation. If the conditions for equation (7c) are not satisified then the original value of τ remains unchanged.

The resulting spin torque about the z axis is then obtained by integrating the elemental moments over the whole contact ellipse as

$$\vec{M}_{s1} = \int d\vec{M}_{s1} = \int y\,\hat{j} \times d\vec{F} \tag{9}$$

In addition to the effect on spinning torque of the lubricant within the Hertzian contact region, the effect of the lubricant outside of this region must be considered. The expression for this moment is given in reference 8 as

$$M_{s2} = 4\mu\omega_s \int_0^{\pi/2} \int_{r_o}^{KR} \frac{r^3\, d\varphi\, dr}{\left(R + h - \frac{R_G}{\cos\varphi}\right) + \left[\left(\frac{R_G}{\cos\varphi}\right)^2 - r^2\right]^{1/2} - \left(R^2 - r^2\right)^{1/2}} \tag{10}$$

This may be integrated numerically over the region outside the contact ellipse. The total moment M_s, is therefore the sum of the moments given by the equations (9) and (10)

$$M_s = M_{s1} + M_{s2} \tag{11}$$

Spinning torques are computed for both inner and outer ball/race contacts and for equilibrium it is necessary for the net vector moment on the ball in the z direction to be zero. Therefore for equilibrium

$$\vec{M}_{si} + \vec{M}_{so} = 0 \tag{12}$$

The value of the spinning torque at the inner and outer ball/race contacts are dependent upon the relative spin velocities which are in turn dependent upon the angle β of the angular velocity vector. In order to obtain the correct value of β, two extreme values are assumed and the net moment on the ball computed for each and an interpolation procedure is used to arrive at that value for which the net moment on the ball is close to zero. The criteria used in the numerical computation is

$$\frac{|\vec{M}_i + \vec{M}_o|}{|\vec{M}_i| + |\vec{M}_o|} < 0.01 \tag{13}$$

When the net moment has been obtained within the limit defined by equation (13), the resulting bearing torque due to ball spinning friction only is obtained as

$$T_1 = NM_s \sin \theta \tag{14}$$

Rolling Resistance

As the ball rolls in the groove, lubricant is squeezed out ahead of the ball/race contact as shown in figure 4(a). However, if inertia effects are neglected, the ball must be in equilibrium and therefore some microslip must be present in order to provide balancing forces F_{si} and F_{so} (fig. 4(c)).

A simple force analysis shows that for equilibrium:

$$F_{si} - F_{so} - F_{Ri} + F_{Ro} = 0 \tag{15}$$

and by taking moments about the center of the ball

$$R(F_{si} - F_{Ri}) - R(F_{so} - F_{Ro}) = 0 \tag{16a}$$

it may be seen that

$$F_{si} = F_{Ri} \tag{16b}$$

$$F_{so} = F_{Ro} \tag{16c}$$

The rolling velocities are obtained from the kinematics outlined in appendix A. The shear force due to rolling is obtainable from the analysis presented in reference 13 and modified for a ball race contact as indicated in appendix C.

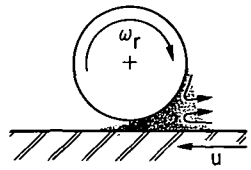

(a) Reverse flow of lubricant in entry region.

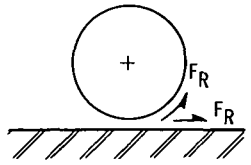

(b) Friction forces on ball and race due to reverse flow.

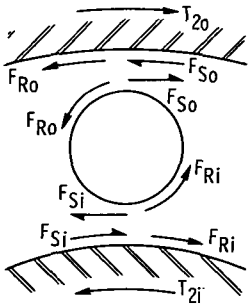

(c) Ball and races showing all forces necessary for equilibrium.

Figure 4. - Origin of rolling drag on ball and race.

The torque on the inner ring due to the rolling resistance is then given by

$$T_{2i} = 2F_{Ri}NR_i \tag{17a}$$

Similarly the torque on the outer ring is given by

$$T_{2o} = 2F_{Ro}NR_o \tag{17b}$$

The preceding analysis is based upon the assumption that the microslip necessary to provide the forces F_{si} and F_{so} is small in comparison with the other motion of the ball/race system and therefore does not significantly change the kinematics of the bearing.

Fluid-Dynamic Drag

As the balls orbit within the bearing there is a drag force present which is approximately equivalent to the drag of a sphere submerged in a fluid. An approximate analysis of this can be made using the following assumptions:

(1) Each ball is assumed to behave as it would while moving in a steady stream of fluid.

(2) Interaction of the balls with each other is neglected.

(3) Any effect due to rotation of the balls is neglected.

On the basis of the preceding assumptions, the drag F_D of a single ball may be computed by the following formula (ref. 14)

$$F_D = C_D \pi R^2 \left(\frac{1}{2} \rho U_c^2\right) \tag{18}$$

A difficulty arises because the density of the medium must be known. The viscosity of the medium also must be known because the drag coefficient C_D is dependent upon the Reynolds number (ref. 14). The fluid in the annular space is, however, not homogeneous but a mixture of air and lubricant.

The drag force may, however be bracketed by computing a value based upon air alone and another value based on the annular space being filled with lubricant.

As shown in figure 5, for equilibrium the drag force must be balanced by forces at the inner and outer ball/race contact. These forces would be caused by microslip at the ball/race contact and would each be equal to $F_D/2$. The resulting torque on the inner race is then

$$T_{3i} = R_i \frac{F_D}{2} \tag{19a}$$

and on the outer race is

$$T_{3o} = R_o \frac{F_D}{2} \tag{19b}$$

The torque at the inner race therefore adds to the friction torque seen by the rotating inner ring. The fluid drag torque on the outer ring, however, acts in the opposite direction to the other torque values previously discussed (see fig. 5). Hence, this value would be subtracted from the other torque values.

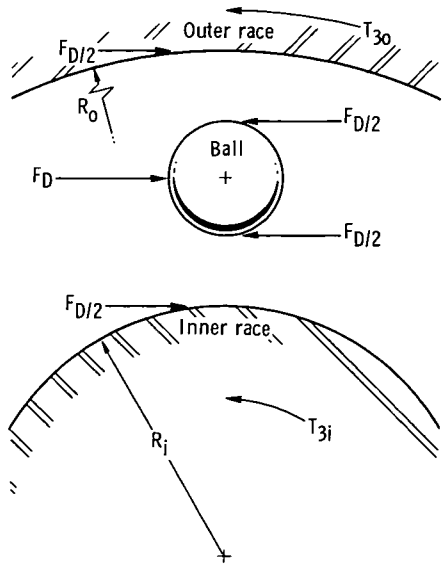

Figure 5. - Fluid dynamic drag on ball and resulting drag forces on inner and outer races.

Hysteresis

When a ball rolls on a plate or in a groove, elastic deformation of the ball and groove will occur. The application and relaxation of load as the ball rolls along the groove will result in a certain amount of hysteresis loss within the stressed zones of the ball and groove.

An experimental investigation of the hysteresis loss for balls rolling on a flat plate is reported in reference 15. A semianalytical relation is reported in reference 15 between the specific damping capacity of the material and the resisting force. This relation is

$$F_H = 0.1315\left(\frac{1}{E_1} + \frac{1}{E_2}\right)\frac{P^2}{a^2} \times \text{Specific damping capacity} \tag{20}$$

For an AISI 52100 steel ball (R_c 60) a value of the specific damping capacity of 0.007 is given in reference 15.

Since the stressed region is assumed to be that enclosed within the Hertzian contact region, equation (20) may be modified for an elliptic contact region similar to that present between a ball and groove by substituting the area of an ellipse for that of a circle. Equation (20) then becomes

$$F_H = 0.1315\left(\frac{1}{E_1} + \frac{1}{E_2}\right)\frac{P^2}{ab} \times \text{Specific damping capacity} \tag{21}$$

The torque on the outer race due to hysteresis is then obtained as

$$T_{4o} = NF_H(R_P + R\cos\theta) \tag{22}$$

Total Friction Torque

Neglecting coupling between the various effects considered individually and combining equations (14), (17b), (19b), and (22) result in the gross torque on the outer race where

$$T_o = T_{1o} + T_{2o} - T_{3o} + T_{4o} \tag{23}$$

RESULTS AND DISCUSSION

The friction torques were measured experimentally for all specimen and lubricant combinations at loads varying from 44.5 to 403 newtons (10 to 90 lb) and for speeds of 1000, 2000, and 3000 rpm. For each lubricant, the torque was measured under conditions of a full supply of lubricant to the bearing and then with a thin film of lubricant, only.

Experimental torque results for the di-2-ethylhexyl sebacate for the 17° and 26° contact angle bearing are shown in figures 6 and 7 for oil jet lubrication. The same tests were repeated for thin film lubrication. However, no significant difference was obtained between the experimental results for the full lubrication condition and the thin film case. The analytical values for the torque due to the combined spinning, rolling, and hysteresis on the outer races are also shown in figures 6 and 7. Calculated values for the fluid-dynamic drag have not been included because of the unknown nature of the fluid within the annular region.

The experimental values of the friction torques of the 17° and 26° contact angle bearing lubricated with the synthetic paraffinic lubricant for oil jet lubrication are shown in figures 8 and 9. The calculated values for the combined spinning and rolling torque are shown in the same figures. There is reasonably good agreement between experimental and analytical values of torque for jet lubrication. The calculated values of torque increase more with speed than do the experimental values. This result is most likely caused by more lubricant being thrown out of the bearing as the speed increases

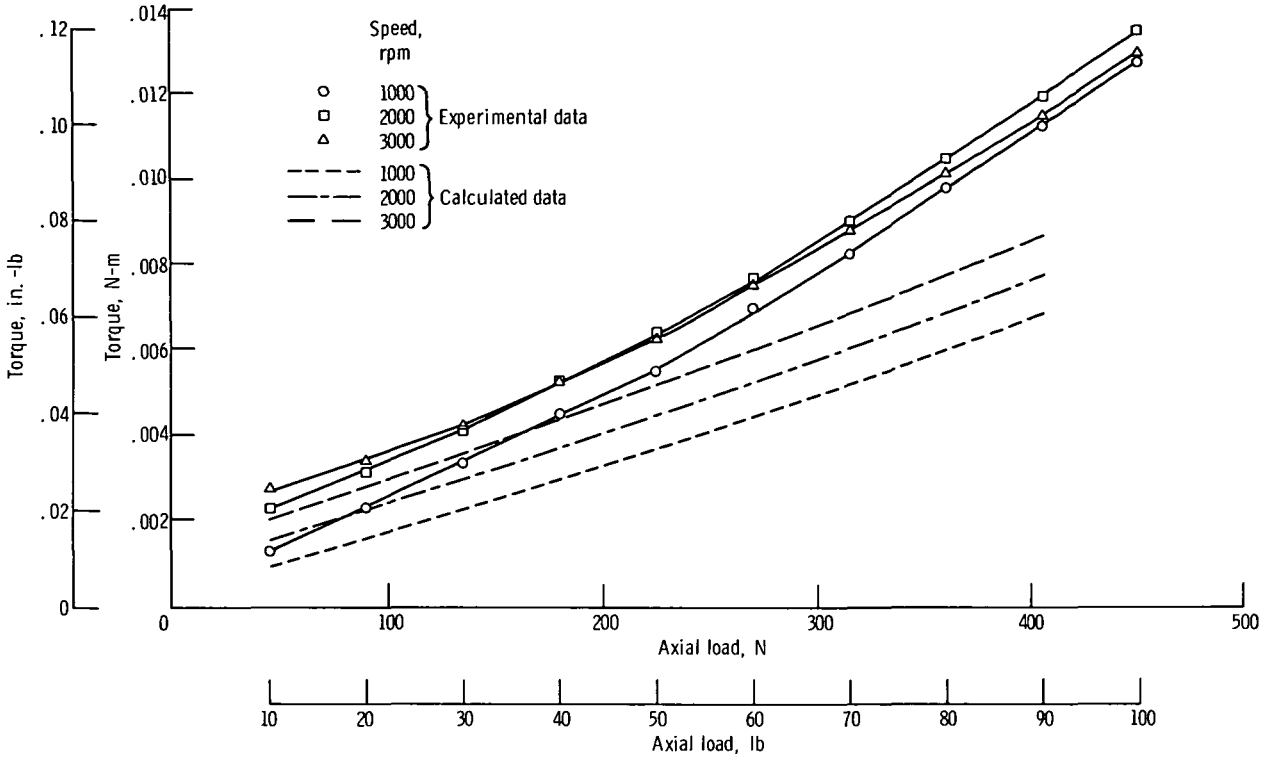

Figure 6. - Experimental and calculated values of torque plotted against load for jet and thin film lubrication with di-2-ethylhexyl sebacate oil. Speed, 1000, 2000, and 3000 rpm; contact angle, 17°; three ball bearings.

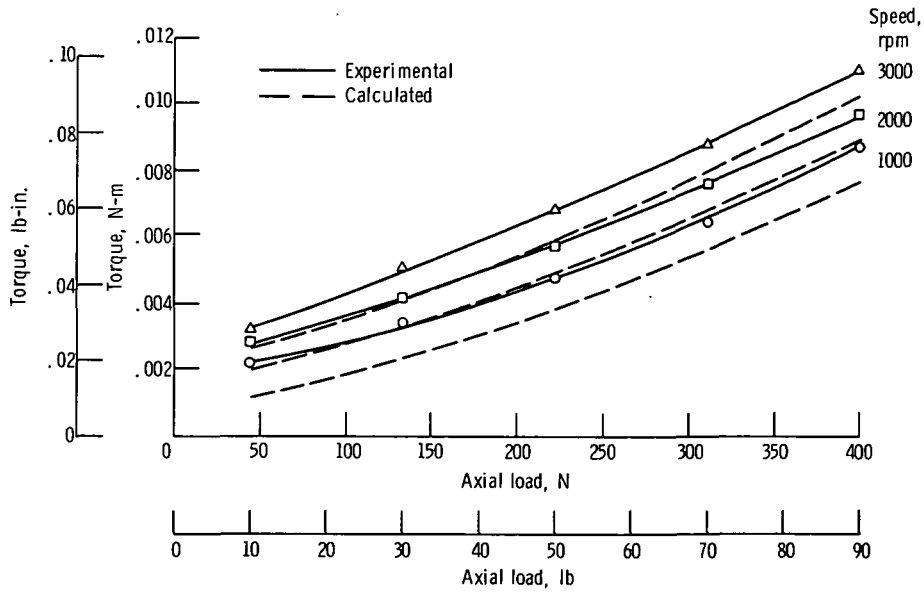

Figure 7. - Comparison of experimental and calculated values of torque plotted against load lubricated with oil jet and thin film di-2-ethylhexyl sebacate. Speed, 1000, 2000, and 3000 rpm; contact angle, 26°; three ball bearings.

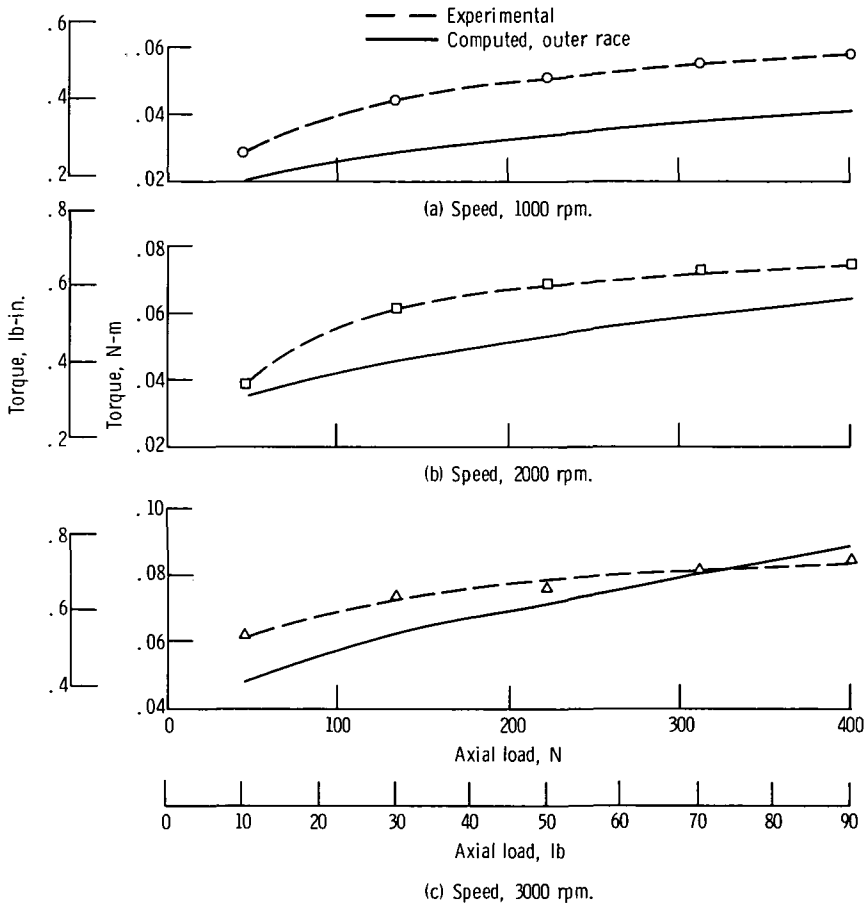

Figure 8. - Experimental and calculated values of torque plotted against load for jet lubrication with synthetic paraffinic oil. Contact angle, 17°; lubricant, 8-cubic-centimeter-per-minute oil jet of synthetic paraffinic oil.

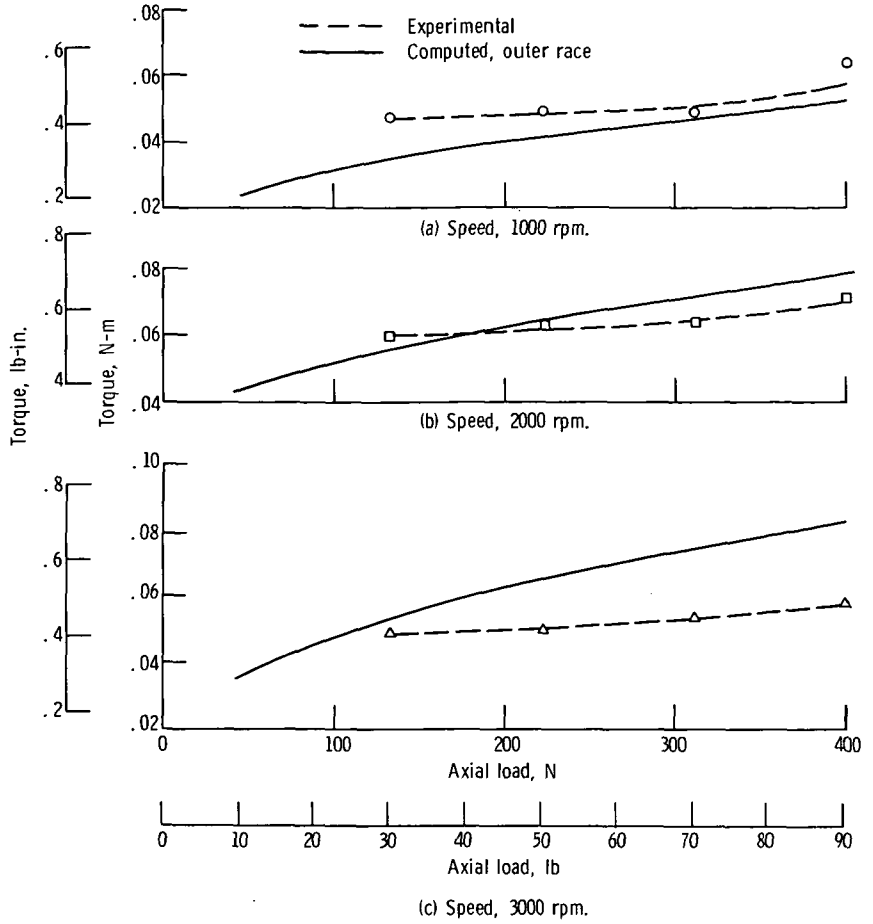

Figure 9. - Experimental and calculated values of torque plotted against load for jet lubrication with synthetic paraffinic oil. Contact angle, 26°; lubricant, 8-cubic-centimeter-per-minute oil jet of synthetic paraffinic oil.

for the experimental case.

Figures 10 and 11 show the experimental results for the thin film lubrication of the synthetic paraffinic oil. From these data it is seen that the speed effect is practically nonexistent. The experimental trend for thin film lubrication values compare reasonably well with the calculated values of torque considering the spinning term (eq. (14)) and hysteresis loss (eq. (22)) only.

In comparing the torque values of figures 8 and 9 with figures 10 and 11, there is an order of magnitude increase in torque with jet lubrication as opposed to thin film lubrication with the synthetic paraffinic lubricant. This increase did not occur with the much less viscous di-2-ethylhexyl sebacate. This is because the di-2-ethylhexyl sebacate which is less viscous than the synthetic paraffinic oil was not retained in the bearing. The small amount of lubricant remaining in the bearing did not cause a measurable increase in the viscous torque of the bearing.

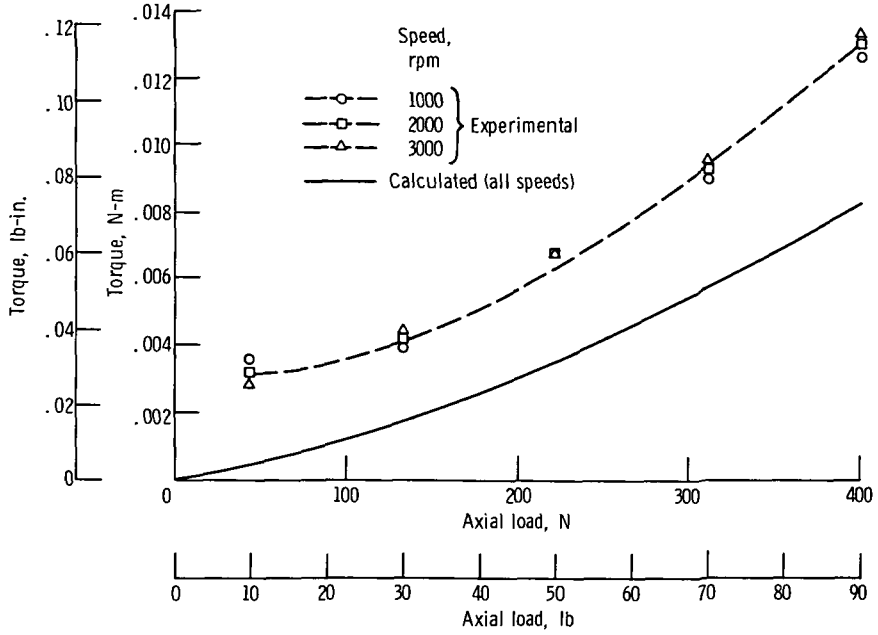

Figure 10. - Experimental and calculated values of torque plotted against load lubricated with thin film of synthetic paraffinic oil. Speed, 1000, 2000, and 3000 rpm; contact angle, 17^{0}.

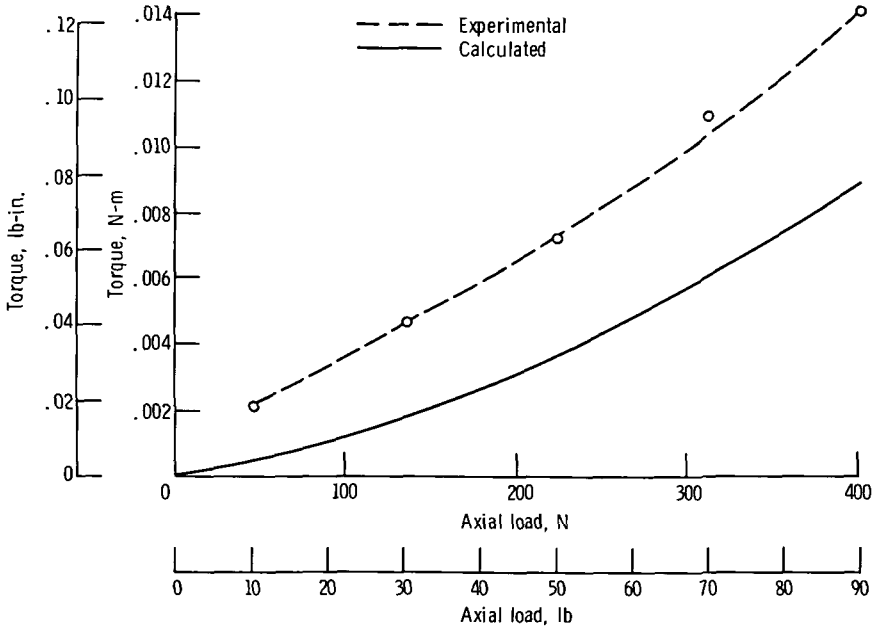

Figure 11. - Comparison of experimental and calculated values of torque at various loads for bearing lubricated with thin film of synthetic paraffinic oil. Speed, 1000, 2000, and 3000 rpm; contact angle, 26^{0}.

TABLE I. - POSSIBLE LIMITING VALUES OF FLUID DYNAMIC DRAG TORQUE BASED ON COMPLETE FILLING OF THE ANNULAR CAVITY WITH A HOMOGENEOUS FLUID

[Ambient room temperature.]

Fluid	Orbital speed, m/sec (in./sec)	Reynolds number, Re	Drag coefficient, C_D	Drag force/ball, N (lb)	Total drag torque, N-m (lb-in.)	Speed, rpm
Air	0.7 (27.5)	327	0.55	6.4×10^{-6} (1.4×10^{-6})	3.2×10^{-7} (2.8×10^{-6})	1000
	2.13 (84)	990	0.42	4.6×10^{-5} (1.0×10^{-5})	2.3×10^{-6} (2×10^{-5})	3000
Di-2-ethylhexyl sebacate	0.7 (27.5)	287	0.7	6.1×10^{-3} (1.4×10^{-3})	3.2×10^{-4} (2.8×10^{-3})	1000
	2.13 (84)	880	0.45	0.037 (0.008)	0.0018 (0.016)	3000
Synthetic paraffinic oil	0.7 (27.5)	10.7	4	0.036 (0.008)	0.0018 (0.016)	1000
	2.13 (84)	33.0	2	0.168 (0.038)	0.0086 (0.076)	3000

The computed minimum and maximum torques expected from the fluid-dynamic drag are shown in table I. This value is arrived at by considering the annular space to be filled with air only. For the other values the space is considered to be completely filled with lubricant. On the basis of drag in air, the contribution to the total bearing torque is insignificant. The assumption of completely filling the annular space with the synthetic paraffinic oil yields a maximum value of 0.008 newton-meter (0.07 lb-in.) at 3000 rpm.

The computed bearing torques due to hysteresis effects only are shown in figure 12. These torques are dependent only upon load and contact angle and are independent of speed and lubricant. However, as shown in figure 12, the hysteresis effect alone is insignificant compared with the other factors considered.

The agreement between the experimental results and the computed values is generally good, although the computed torque is, with few exceptions, less than the corresponding experimental value. In all cases, an extrapolation of the curves back to the zero load point yields a finite torque at the no-load condition. This is to be expected in the case of the di-2-ethylhexyl sebacate and the synthetic paraffinic lubricants with adequate lubricant supply because the rolling term will still be present with zero load.

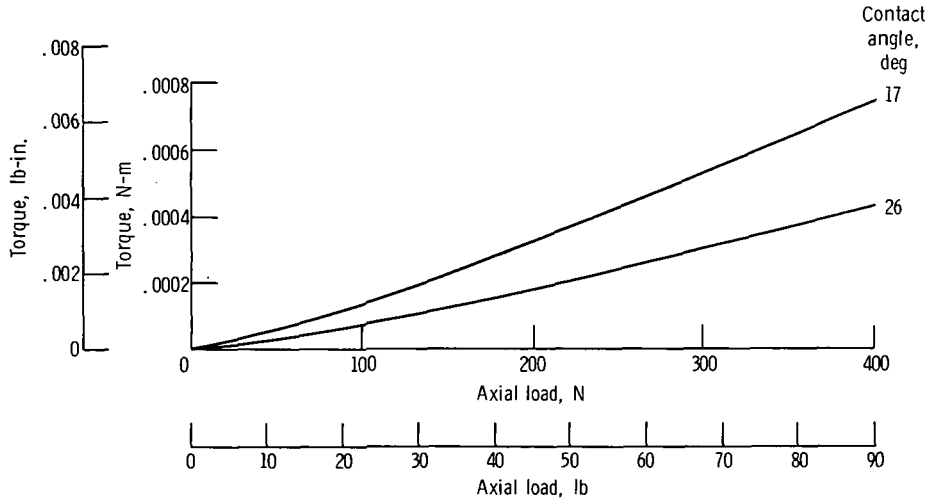

Figure 12. - Hysteresis torques for 17° and 26° contact angle bearings with three balls.

However, for the case of the thin film, the only torques computed are those due to the ball spin and hysteresis effects. There would, however, be a small rolling torque with any nonzero lubricant film. This small rolling torque undoubtedly accounts for the small torque present at zero load which would have the effect of raising the computed value by approximately the same amount over the whole load range, bringing the computed and experimental values into close agreement.

SUMMARY OF RESULTS

The NASA spinning torque apparatus was modified to measure the spinning torque on a cageless ball thrust bearing. Friction torque was measured for thrust loads varying from 44.5 to 403 newtons (10 to 90 lb) at speeds of 1000, 2000, and 3000 rpm. Tests were conducted with di-2-ethylhexyl sebacate and a synthetic paraffinic oil. These tests were run with either oil jet lubrication or with a thin surface film of lubricant. An analytical model which included rolling resistance was developed and extended from a previous model for spinning torque and lubricant rheology. The following results were obtained:

1. The bearing analytical model and lubricant rheological model developed for determining the friction torques in a thrust loaded ball bearing are confirmed by fair agreement between the computed and experimental results.

2. For a lubricant of relatively low viscosity such as di-2-ethylhexyl sebacate, the largest contribution to the friction torque is the ball spinning component. The torque appears to be relatively unaffected by the amount of lubricant present.

3. For a viscous lubricant such as the synthetic paraffinic oil, the largest contribution to friction torque is that of the rolling resistance of the ball through the lubricant. In this case, a reduction of the amount of lubricant present appreciably reduces the friction torque. With only a thin film, the contribution of the rolling resistance disappears altogether.

4. With a low viscosity lubricant, an excess amount of lubricant present in the bearing has little deleterious effect. However, with a viscous lubricant, a nominal flow of oil to the bearing can result in a tenfold increase in the friction torque as compared with the minimum value.

Lewis Research Center,
National Aeronautics and Space Administration,
Cleveland, Ohio, April 4, 1973,
501-24.

APPENDIX A

SYMBOLS

a	major semiaxis of contact ellipse, m (in.)
a'	minor semiaxis of contact ellipse, m (in.)
B	total curvature
b	semiwidth of contact ellipse at y, m (in.)
C_D	drag coefficient
E'	materials properties factor, N/m^2 (psi)
$E_{1,2}$	modulus of elasticity, N/m^2 (psi)
$\hat{e}$	unit vector along bearing axis
F	lubricant factor
F_a	bearing thrust load, N (lb)
F_D	fluid dynamic drag, N (lb)
F_R	friction force due to rolling drag, N (lb)
F'	function defined by eq. (D2)
F'_R	rolling drag per unit length for cylinder, N (lb)
f	race curvature
h	film thickness, m (in.)
h_o	minimum distance between ball and groove, m (in.)
$\hat{i}, \hat{j}, \hat{k}$	unit vector in x, y, and z direction
K	constant defining outer boundary of integration
K'	function defined by eq. (C2)
$\vec{M}_S$	total spinning torque at ball/race interface
M_{s1}	total spinning torque in Hertzian ellipse, N-m (lb-in.)
M_{s2}	spinning torque due to viscous drag outside Hertzian ellipse, N-m (lb-in.)
N	number of balls
P	normal load, N (lb)

q	reduced pressure
R	radius of ball, m (in.)
R_e	radius of equivalent cylinder, m (in.)
R_g	radius of groove, m (in.)
R_p	pitch radius, m (in.)
R_R	radius of race, m (in.)
r	polar coordinate
r_o	value of r at outer boundary of Hertzian ellipse, m (in.)
S	contact stress, N/m^2 (psi)
T_1	bearing torque due to ball spin torque, N-m (lb-in.)
T_2	bearing torque due to rolling drag, N-m (lb-in.)
T_3	bearing torque due to aerodynamic drag, N-m (lb-in.)
T_4	torque due to hysteresis, N-m (lb-in.)
T_5	total bearing torque, N-m (lb-in.)
U_B	surface velocity of ball relative to moving coordinate system, m/sec (in./sec)
U_C	linear velocity of ball center, m/sec (in./sec)
U_R	surface velocity of race relative to moving coordinate system, m/sec (in./sec)
U_S	relative slip velocity between ball and race, m/sec (in./sec)
W	load per unit width, N/m (lb/in.)
X, Y, Z	Cartesian coordinates, m (in.)
x, y, z	moving coordinate system
α	pressure-viscosity exponent, $(N/m^2)^{-1}$ (psi^{-1})
β	angle which ball angular velocity vector makes with bearing axis, deg
θ	loaded contact angle, deg
θ_o	unloaded contact angle, deg
μ	absolute viscosity, $N\text{-}sec/m^2$ $(lb\text{-}sec/in.^2)$
μ_o	ambient viscosity, $N\text{-}sec/m^2$ $(lb\text{-}sec/in.^2)$
ν	Poisson's ratio
ρ	density of fluid, kg/m^3 $(lb\text{-}sec^2/in.^4)$
τ	shear stress, N/m^2 (psi)

τ' dummy variable

τ_c transition shear stress, N/m^2 (psi)

Φ nondimensional variable denoting distance to location of ambient pressure point

φ polar coordinate in x-y plane

Ω_c angular velocity of ball center, rad/sec

Ω_i angular velocity of inner race, rad/sec

Ω_o angular velocity of outer race, rad/sec

ω angular velocity of ball with respect to rotating coordinate system, rad/sec

ω_i relative angular velocity of inner race with respect to moving coordinate system, rad/sec

ω_o relative angular velocity of outer race with respect to moving coordinate system, rad/sec

ω_r angular velocity of rolling, rad/sec

ω_s angular velocity of spinning, rad/sec

Subscripts:

i inner race

o outer race

Superscript:

$\rightarrow$ denotes vector

APPENDIX B

BEARING KINEMATICS

Kinematics of the ball and races will be considered in relation to a coordinate system X, Y, Z with origin at the ball center and rotating at the orbital angular velocity. The coordinate system is orientated with the z axis along the line of contact as shown in figure 2. The angular velocity $\vec{\omega}$ of the ball with respect to the moving coordinate system is orientated at an angle β to the axis of the bearing.

The unit vector along the bearing axis is $\hat{e}$

$$\hat{e} = \hat{j} \cos \theta - \hat{k} \sin \theta \tag{B1}$$

and the various angular velocities are

$\Omega_i \hat{e}$ angular velocity of inner ring

$\Omega_i \hat{e}$ orbital angular velocity of ball center

$$\vec{\omega} = \omega\left[\hat{j} \cos (\beta - \theta) + \hat{k} \sin (\beta - \theta)\right] \tag{B2}$$

The absolute angular velocity of the ball $\vec{\Omega}_B$ is given by

$$\vec{\Omega}_B = \vec{\omega} + \vec{\Omega}_c \tag{B3}$$

Assuming that no slip occurs at the nominal ball/race contact points the following relation between ω and Ω_c is obtained:

$$\omega = -\frac{R_P + R \cos \theta}{R \cos (\beta - \theta)} \Omega_c \tag{B4}$$

and Ω_c is found in terms of Ω_i as:

$$\Omega_c = \frac{\Omega_i}{2}\left(1 - \frac{R}{R_P} \cos \theta\right) \tag{B5}$$

The angular velocities of the inner race $\vec{\omega}_i$ and outer race $\vec{\omega}_o$ with respect to the rotating coordinate system are

(B6)

$$\vec{\omega}_i = \vec{\Omega}_i - \vec{\Omega}_c = \frac{\Omega_i}{2}\left(1 + \frac{R}{R_p}\cos\theta\right)\hat{e}$$

(B7)

$$\vec{\omega}_o = 0 - \vec{\Omega}_c = -\frac{\Omega_i}{2}\left(1 - \frac{R}{R_p}\cos\theta\right)\hat{e}$$

The angular spin velocities of the ball with respect to the inner and outer races are

(B8a)

$$\omega_{si} = (\vec{\omega} - \vec{\omega}_i) \cdot \hat{k}$$

(B8b)

$$\omega_{si} = \frac{\Omega_i}{2}\left(1 + \frac{R}{R_p}\cos\theta\right)\left[\left(\cos\theta - \frac{R_p}{R}\right)\tan(\beta - \theta) + \sin\theta\right]$$

(B9a)

$$\omega_{so} = (\vec{\omega} - \vec{\omega}_o) \cdot \hat{k}$$

(B9b)

$$\omega_{so} = -\frac{\Omega_i}{2}\left(1 - \frac{R}{R_p}\cos\theta\right)\left[\left(\cos\theta + \frac{R_p}{R}\right)\tan(\beta - \theta) + \sin\theta\right]$$

Finally the angular velocity of rolling of the ball with respect to the reference coordinate system is obtained as

(B10a)

$$\omega_R = \vec{\omega} \cdot \hat{j}$$

(B10b)

$$\omega_R = \omega\cos(\beta - \theta)$$

Surface velocities of the ball and race relative to the moving coordinate system are obtained as

(B11)

$$U_{Bi} = -\left(\omega_{ri}R + \omega_{si}y\right)$$

(B12

$$U_{Bo} = \left(\omega_{ro}R - \omega_{so}y\right)$$

$$U_{Ri} = \omega_{Ri} R \tag{B13}$$

$$U_{Ro} = \omega_{Ro} R \tag{B14}$$

APPENDIX C

CONTACT ANGLE

The loaded contact angle may be computed by the Newton-Raphson method using the iterative equation (ref. 16, p. 159)

$$\theta' = \theta + \frac{\frac{F_a}{4NR^2K'} - \sin\theta\left(\frac{\cos\theta_o}{\cos\theta} - 1\right)^{1.5}}{\cos\theta\left(\frac{\cos\theta_o}{\cos\theta} - 1\right) + 1.5\tan^2\theta\left(\frac{\cos\theta_o}{\cos\theta} - 1\right)^{0.5}\cos\theta_o} \tag{C1}$$

where K' is a function of the curvature of the bearing. A chart of K' as a function of curvature is given in reference 17 (chart 57). This may be approximated by

$$K' = 5.12202\times10^6\, B^{1.18843} \tag{C2}$$

where

$$B = f_i + f_o - 1$$

APPENDIX D

ROLLING RESISTANCE

At the entry region to an EHD contact there is a reverse flow of the lubricant because a portion of the film ahead of the rolling element is squeezed out forward relative to the rolling (ref. 18). This forward flow produces a shear stress on the rolling element and race. An analysis of the resulting rolling traction is presented in reference 14 and for a roller of unit width the rolling drag F'_R is obtained as

$$F'_R = \frac{h}{2\alpha}\left[F'\right]_0^{a'\Phi_i} \tag{D1}$$

where the function F' is an integral evaluated between the limits from the entry to the EHD contact region to the point of ambient pressure in the entry film.

$$\left[F'\right]_0^{a'\Phi_i} = \frac{C}{\left[I\right]_0^{a'\Phi_i}} \int_0^{a'\Phi_i} \frac{\tau'^{3/2}\, d\tau'}{(1 - 2q)\left(1 + \tau'^{3/2}\right)^2} + \ln(1 - c) \tag{D2}$$

where τ' is a dummy variable which is a function of Φ and the reduced pressure q is also a function of Φ. Φ itself is a nondimensional coordinate denoting distance in front of the EHD contact region. Values of the integral $\left[I\right]_0^{a'\Phi_i}$ are tabulated in reference 14 and for large values of Φ_i the value of the integral approach is an asymptote of approximately 0.269.

The function $\left[F'\right]_0^{a'\Phi_i}$ has been evaluated numerically and the value obtained for a thick film, that is, where the ambient pressure is a large distance in front of the entry to the Hertzian region, is $\left[F'\right]_0^{a'\Phi_i} = 11.75$.

Assuming that the analysis can be applied to the elemental rollers comprising the ball/race contact, the rolling drag on the ball and race is then obtained

$$F_R = \int dF_R = \int F'_R\, dy \tag{D3}$$

If the film thickness is assumed to be large so that the values of $\left[I\right]_0^{a'\Phi_i}$ and $\left[F'\right]_0^{a'\Phi_i}$ are approaching the limits as Φ gets large, then the aforementioned integrals approach constant values and the rolling resistance may be written as

$$F_R = \frac{\left[F'\right]_0^{a'\Phi_i}}{2\alpha} \int_{-a}^{a} h \, dy \qquad \text{(D4)}$$

Since the values of h are computed to find the spinning torque, computation of F_R is simply effected by integrating these values of h numerically over the Hertzian contact region.

REFERENCES

1. Poritsky, H.; Hewlett, C. W., Jr.; and Coleman, R. E., Jr.: Sliding Friction of Ball Bearings of the Pivot Type. J. Appl. Mech., vol. 14, no. 4, Dec. 1947, pp. 261-268.

2. Jones, A. B.: Ball Motion and Sliding Friction in Ball Bearings. J. Basic Eng., vol. 81, no. 1, Mar. 1959, pp. 1-12.

3. Reichenbach, G. S.: The Importance of Spinning of Friction in Thrust-Carrying Ball Bearings. J. Basic Eng., vol. 82, no. 2, June 1960, pp. 295-301.

4. Harris, T. A.: Ball Motion in Thrust-Loaded, Angular Contact Bearings with Coulomb Friction. J. Lub. Tech., vol. 93, no. 1, Jan. 1971, pp. 32-38.

5. Harris, T. A.: An Analytical Method to Prevent Skidding in Thrust-Loaded Angular-Contact Ball Bearings. J. Lub. Tech., vol. 93, no. 1, Jan. 1971. pp. 17-24.

6. Miller, Steven T.; Parker, Richard J.; and Zaretsky, Erwin V.: Apparatus for Studying Ball Spinning Friction. NASA TN D-2796, 1965.

7. Dietrich, Marshal W.; Parker, Richard J.; and Zaretsky, Erwin V.: Effect of Ball-Race Conformity on Spinning Friction. NASA TN D-4669, 1968.

8. Dietrich, M. W.; Parker, R. J.; Zaretsky, E. V.; and Anderson, W. J.: Contact Conformity Effects on Spinning Torque and Friction. J. Lub. Tech., vol. 91, no. 2, Apr. 1969, pp. 308-313.

9. Allen, C. W.; Townsend, D. P.; and Zaretsky, E. V.: Elastohydrodynamic Lubrication of a Spinning Ball in a Nonconforming Groove. J. Lub. Tech., vol. 92, no. 1, Jan. 1970, pp. 89-96.

10. Allen, Charles W.; Townsend, Dennis P.; and Zaretsky, Erwin V.: Comparison of Conventional and Microasperity Elastohydrodynamic Lubrication of a Ball Spinning in a Nonconforming Groove. NASA TN D-6761, 1972.

11. Allen, Charles W.; Townsend, Dennis P.; and Zaretsky, Erwin V.: New Generalized Rheological Model for Lubrication of a Ball Spinning in a Nonconforming Groove. NASA TN D-7280, 1973.

12. Dowson, D. and Higginson, G. R.: Elasto-hydrodynamic Lubrication. Pergamon Press, 1966.

13. Wolveridge, P. E.; Baglin, K. P.; and Archard, J. F.: The Starved Lubrication of Cylinders in Line Contact. Proc. Inst. Mech. Eng., vol. 185, no. 81/71, 1970-71, pp. 1159-1169.

14. Eskinazi, Salamon: Principles of Fluid Mechanics. Second ed., Allyn and Bacon, 1962, p. 438.

15. Drutowski, R. C.: Energy Losses of Balls Rolling on Plates. J. Basic Eng., vol. 81, no. 2, June 1959, pp. 233-238.

16. Harris, Tedric A.: Rolling Bearing Analysis. John Wiley & Sons, Inc., 1966.

17. Jones, A. B.: Analysis of Stresses and Deflections. Vol. 21, New Departure Div., General Motors Corp., 1946.

18. Cheng, H. S.: Calculation of Elastohydrodynamic Film Thickness in High Speed Rolling and Sliding Contacts. Rep. MTI-67TR24, Mechancial Technology, Inc. (AD-652924), May 1967.

NATIONAL AERONAUTICS AND SPACE ADMINISTRATION
WASHINGTON, D.C. 20546

OFFICIAL BUSINESS
PENALTY FOR PRIVATE USE $300

SPECIAL FOURTH-CLASS RATE
BOOK

POSTAGE AND FEES PAID
NATIONAL AERONAUTICS AND
SPACE ADMINISTRATION
451

U.S.MAIL

POSTMASTER : If Undeliverable (Section 158 Postal Manual) Do Not Return

"The aeronautical and space activities of the United States shall be conducted so as to contribute . . . to the expansion of human knowledge of phenomena in the atmosphere and space. The Administration shall provide for the widest practicable and appropriate dissemination of information concerning its activities and the results thereof."

—NATIONAL AERONAUTICS AND SPACE ACT OF 1958

NASA SCIENTIFIC AND TECHNICAL PUBLICATIONS

TECHNICAL REPORTS: Scientific and technical information considered important, complete, and a lasting contribution to existing knowledge.

TECHNICAL NOTES: Information less broad in scope but nevertheless of importance as a contribution to existing knowledge.

TECHNICAL MEMORANDUMS: Information receiving limited distribution because of preliminary data, security classification, or other reasons. Also includes conference proceedings with either limited or unlimited distribution.

CONTRACTOR REPORTS: Scientific and technical information generated under a NASA contract or grant and considered an important contribution to existing knowledge.

TECHNICAL TRANSLATIONS: Information published in a foreign language considered to merit NASA distribution in English.

SPECIAL PUBLICATIONS: Information derived from or of value to NASA activities. Publications include final reports of major projects, monographs, data compilations, handbooks, sourcebooks, and special bibliographies.

TECHNOLOGY UTILIZATION PUBLICATIONS: Information on technology used by NASA that may be of particular interest in commercial and other non-aerospace applications. Publications include Tech Briefs, Technology Utilization Reports and Technology Surveys.

Details on the availability of these publications may be obtained from:

SCIENTIFIC AND TECHNICAL INFORMATION OFFICE

NATIONAL AERONAUTICS AND SPACE ADMINISTRATION

Washington, D.C. 20546